



How Baleen Whales Feed: The Biomechanics of Engulfment and Filtration

J.A. Goldbogen,¹ D. Cade,¹ J. Calambokidis,²
A.S. Friedlaender,³ J. Potvin,⁴ P.S. Segre,¹
and A.J. Werth⁵

¹Department of Biology, Hopkins Marine Station, Stanford University, Pacific Grove, California 93950; email: jergold@stanford.edu, davecade@stanford.edu, psegre@stanford.edu

²Cascadia Research Collective, Olympia, Washington 98501; email: calambokidis@cascadiaresearch.org

³Marine Mammal Institute, Hatfield Marine Science Center, Oregon State University, Newport, Oregon 97365; email: ari.friedlaender@oregonstate.edu

⁴Department of Physics, Saint Louis University, St. Louis, Missouri 63103; email: potvinj@slu.edu

⁵Department of Biology, Hampden-Sydney College, Hampden-Sydney, Virginia 23943; email: awerth@hsc.edu

Annu. Rev. Mar. Sci. 2017. 9:11.1–11.20

The *Annual Review of Marine Science* is online at marine.annualreviews.org

This article's doi:
10.1146/annurev-marine-122414-033905

Copyright © 2017 by Annual Reviews.
All rights reserved

Keywords

Mysticeti, baleen, filtration, drag, whale, feeding

Abstract

Baleen whales are gigantic obligate filter feeders that exploit aggregations of small-bodied prey in littoral, epipelagic, and mesopelagic ecosystems. At the extreme of maximum body size observed among mammals, baleen whales exhibit a unique combination of high overall energetic demands and low mass-specific metabolic rates. As a result, most baleen whale species have evolved filter-feeding mechanisms and foraging strategies that take advantage of seasonally abundant yet patchily and ephemerally distributed prey resources. New methodologies consisting of multi-sensor tags, active acoustic prey mapping, and hydrodynamic modeling have revolutionized our ability to study the physiology and ecology of baleen whale feeding mechanisms. Here, we review the current state of the field by exploring several hypotheses that aim to explain how baleen whales feed. Despite significant advances, major questions remain about the processes that underlie these extreme feeding mechanisms, which enabled the evolution of the largest animals of all time.

INTRODUCTION

How animals enhance survival and fitness by optimizing resource acquisition and utilization is a central question that spans the disciplines of physiology, behavior, evolution, and ecology (Charnov 1976, Pyke 1984, Smith 1978). The study of foraging energetics requires a detailed understanding of the mechanisms and processes that determine prey selection, predator-prey interactions, and feeding performance (Mori 1998, 2002). Models of feeding physiology and foraging ecology are integrative in nature and require a detailed understanding of energetic expenditures, the biomechanics of prey capture and assimilation, and the abundance and distribution of prey. Quantifying these parameters in a dynamic natural environment can be challenging, and therefore basic models of foraging ecology are lacking for many animal systems.

The Krogh principle states that among the great diversity of animals there will be one that is best suited as an experimental system for any biological problem (Krogh 1929). Here, we argue that the unique foraging adaptations that characterize baleen whales (Mysticeti) present an exceptional and powerful system for the study of feeding biomechanics and physiological ecology. Moreover, we invoke the principles of exploratory and comparative physiology (Somero 2000) to reveal how the foraging adaptations of mysticetes inform our understanding of animal function at the upper extreme of body mass and potentially the physiological limitations to large size (Alexander 1998). Given that several species of extant mysticetes are the largest animals of all time, we are truly living in a time of giants, and this presents a unique opportunity to study the physiological ecology of extreme body size.

The advantage of using baleen whale foraging as a model system to address broad biological questions stems from recent technological advances in remote sensing and biologging tags (Goldbogen & Meir 2014, Johnson & Tyack 2003). Although baleen whale anatomy has been studied for more than a century (Eschricht & Reinhardt 1866, Goldbogen et al. 2015b), only recently have investigators been able to develop a more quantitative understanding of the physiological and ecological processes associated with this unique ecomorphology and life history (Goldbogen et al. 2013b, Pyenson et al. 2012). The advent of animal-borne tags equipped with a suite of movement, audio, and video sensors has changed the way we think about cetacean biology because it enables the quantification of foraging performance at high resolution (Aoki et al. 2012; Simon et al. 2009, 2012). Tagging studies can be coordinated with the use of scientific echo sounders to measure the abundance, distribution, and density of prey where whales forage (Friedlaender et al. 2009, 2013; Hazen et al. 2009). By integrating these data, comparative studies reveal how baleen whales exploit dynamic, heterogeneous prey fields through changes in locomotor behavior and feeding performance (Friedlaender et al. 2013, Hazen et al. 2015). Moreover, the incorporation of these data sets into hydromechanical models provides researchers with a powerful tool to explore the energetic consequences and constraints of gigantic filter feeders (Goldbogen et al. 2011, Potvin et al. 2012).

Baleen whales (Mysticeti) are edentulous predators that evolved from toothed whales (Odontoceti) in order to more efficiently feed on aggregations of small-bodied prey using an oral filter (Demere et al. 2008; Fitzgerald 2006, 2012). Instead of teeth, baleen whales have bilaterally symmetric racks of keratinized plates that extend down from the top of the inside of the mouth (Ekdale et al. 2015, Szewciw et al. 2010, Young et al. 2015). The medial margins of baleen plates fray to expose millimeter-scale tubules, or fringes, that interlock to form a dense fibrous mat (Fudge et al. 2009, Pivorunas 1979, Williamson 1973). This dense mat of baleen fringes acts as a filter for engulfed water exiting the mouth, leaving prey inside the mouth for swallowing (Werth 2001, 2011; Werth & Potvin 2016). Although it is recognized that mysticetes use baleen to filter prey suspended in engulfed water, the precise hydrodynamic mechanisms employed during

filtration are only now being rigorously tested experimentally (Werth 2004, 2011; Werth & Potvin 2016; Werth et al. 2016).

Extant baleen whales use one of three recognized modes of filter feeding (Werth 2000): continuous ram filter feeding, used by bowhead and right whales (Balaenidae); intermittent ram filter feeding or lunge feeding, used by rorqual whales (Balaenopteridae); and suction filter feeding, used by gray whales (Eschrichtiidae, with a single extant species, *Eschrichtius robustus*). Balaenids use their forward locomotion to drive prey-laden water into their mouth, causing it to flow past and through the baleen system, to emerge free of prey items through an opening located at the posterior end of the engulfment apparatus (Werth 2004, Werth & Potvin 2016). By contrast, lunge feeding in balaenopterids occurs as a sequential two-step process that begins with the engulfment of a discrete but large volume of prey-laden water during a high-velocity lunge, and ends with the purging and filtration of the water out of the distended buccal cavity (Goldbogen 2010, Goldbogen et al. 2007).

Suction feeding has been documented as a primary feeding mode only in eschrichtiids, who use it to target benthic prey (Johnson & Nelson 1984, Nerini 1984, Ray & Schevill 1974, Woodward & Winn 2006). However, eschrichtiids have also been known to use ram feeding while foraging at different locations in the water column (Nerini 1984, Pyenson & Lindberg 2011). Almost nothing is known about feeding in the pygmy right whale, *Caperea marginata* (Neobalaenidae), one of the smallest mysticetes, which is now thought to be a relic of the otherwise extinct cetothere lineage (Fordyce & Marx 2013). Although this enigmatic species is more closely related to rorquals than to right whales, its name derives from its arched jawline and semicircular lower lip, both of which are reminiscent of those in balaenids.

The morphological and kinematic diversity across mysticetes likely reflects selection pressures associated with the hydrodynamics of engulfment and filtration of different feeding modes and their preferred prey types. Moreover, the diversity and disparity of feeding mechanisms among mysticetes suggest a similarly wide range of energetic strategies and ecological niches. However, all bulk filter-feeding modes in mysticetes are fundamentally different from the dominant feeding modes in odontocetes, which are characterized by the use of raptorial or suction-aided capture of single prey using echolocation (Bloodworth & Marshall 2005, Kane & Marshall 2009, Madsen et al. 2013, Miller et al. 2004). It is often hypothesized that bulk filter feeding is energetically more efficient than particulate feeding, and that this difference in overall foraging efficiency is reflected in the evolution of body size differences among extant cetaceans. Despite several lineages of toothed whales exhibiting gigantism, such as sperm whales (Physeteridae) and some beaked whale species (Ziphiidae), the average body size of mysticetes is greater than that of odontocetes, and the largest mysticetes are far larger than the largest odontocetes (Lindberg et al. 2006, Lockyer 1976). The ability of mysticetes to rapidly increase lipid reserves during a foraging season is a further testament to their high foraging efficiency (Brodie 1975, Williams et al. 2013). Intensified feeding on seasonally abundant prey to build up large lipid reserves for long-distance migration and long-term fasting is a hallmark of baleen whale life history and physiological ecology. Although large body size confers low mass-specific metabolic rates and an economical cost of transport (Williams 1999), mysticetes predictably have high absolute metabolic rates associated with gigantism, carnivory, and a fully aquatic existence (Lockyer 1981, Williams 2006, Williams et al. 2001). Moreover, baleen whales must meet these extraordinary metabolic demands by feeding on relatively small prey items that are several orders of magnitude smaller than their own body (Domenici 2001). Therefore, the study of baleen whale feeding mechanisms provides a fundamental and critical insight into organismal function at the largest absolute scale as well as an extreme predator-prey size differential.

BIOMECHANICS OF BALEEN WHALE FEEDING

Recent research on baleen whale feeding has focused primarily on two families: Balaenidae and Balaenopteridae. Although both of these families rely on filter feeding, they have radically different engulfment apparatuses, filtration mechanisms, and ecological niches. Balaenids engulf and filter feed at low travel speeds ($<1 \text{ m s}^{-1}$), whereas rorquals engulf at significantly higher speeds ($\sim 2\text{--}5 \text{ m s}^{-1}$), thereby incurring greater mass-specific energy and power expenditures. Because of these basic differences, filter feeding by Balaenidae has been broadly categorized as marine grazing (Hazen et al. 2015), whereas lunge filter feeding by Balaenopteridae is more raptorial in nature with respect to the dynamics of predator and prey (Potvin et al. 2010).

Balaenidae

Although the continuous ram filter-feeding mechanism in balaenids (the bowhead whale, *Balaena mysticetus*, and three right whale species of the genus *Eubalaena*) is different from that of other baleen whales (Werth 2004), it is similar in many ways to the unidirectional filter-feeding modes documented in other marine vertebrates, such as whale sharks and manta rays (Motta et al. 2010; Paig-Tran et al. 2011, 2013). Balaenids continuously filter feed at slow swimming speeds, in extended bouts lasting up to several minutes, from dense patches of plankton at the surface or other levels of the water column (Baumgartner et al. 2003, Parks et al. 2012, Simon et al. 2009). This ram-driven filtration process operates much like a plankton tow net except that the baleen filter in the mouth is propelled forward by the whale's forward locomotion (Figures 1 and 2). Balaenid baleen is notable for its extreme length, with plates reaching more than 4 m in length, and for its very fine fringe hairs (diameter $< 0.25 \text{ mm}$) (Lambertsen et al. 2005, Werth 2011). Other features of balaenid anatomy (Werth 2001, 2007)—especially a prominent midline gap between left and right baleen racks; a high, arched rostrum; large, semicircular lips; and a gutter-like groove between the lip and baleen rack—all contribute to continuous water flow through the mouth, which presumably also aids in thermoregulation as large amounts of cold water flow past a highly vascularized palatal organ (Ford et al. 2013).

Data from tagged bowhead whales (Simon et al. 2009) revealed ram feeding at depths of 100 m at the bottom of U-shaped, 15–20-min breath-holding dives, with 2–3-min interludes of open gape, as indicated by slowed forward progress caused by increased drag generation from filtration. Unlike the stroke-and-glide gait used by other marine mammals to save energy (Williams 2001), tagged bowheads used a steady, faster fluking rate (0.12 Hz, significantly higher than the fluke rate during descent and ascent), with a total forward swim speed during filtration of approximately 0.7 m s^{-1} during ram filtration. Simon et al. (2009) hypothesized that this translates to a sixfold increase in total drag generation during foraging (i.e., when the mouth is open to expose the baleen filter); they interpreted the occasional brief pauses in swimming, occurring roughly every 2.5 min during forward locomotion within a prey field, as relating to mouth closure and the consequent swallowing of accumulated prey. Further support for such high drag estimates (two to five times those of non-feeding travel) was obtained from tagging and hydrodynamic modeling studies in North Atlantic right whales (Nousek-McGregor 2010).

Werth (2004) estimated the size of the mouth aperture in feeding adult bowhead whales as 4.23 m^2 . Applying this size to tag data that indicate a swim speed during filtration of 0.8 m s^{-1} during feeding yields a filtration rate of roughly $3.2 \text{ m}^3 \text{ s}^{-1}$, with a consequent estimated daily filtering rate of approximately $80,000 \text{ m}^3$ of water per whale. Previous calculations suggested that, given a copepod density of 0.001 kg m^{-3} (Laidre et al. 2007), bowheads would need to filter $800,000 \text{ m}^3$ per day to meet basic energetic demands, which would mean that a whale foraging for 7 h per day would need to capture prey at speeds of 7.5 m s^{-1} —10 times the observed speed, with

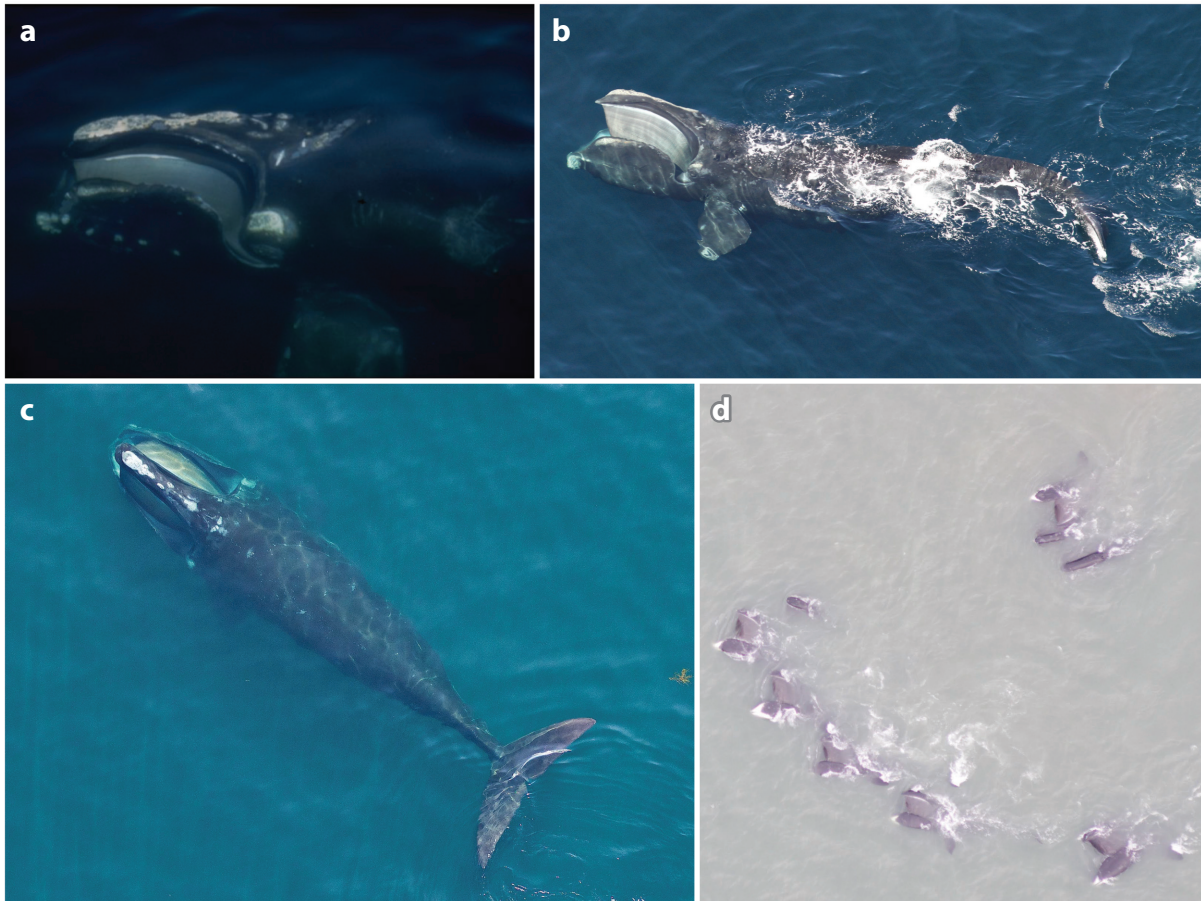


Figure 1

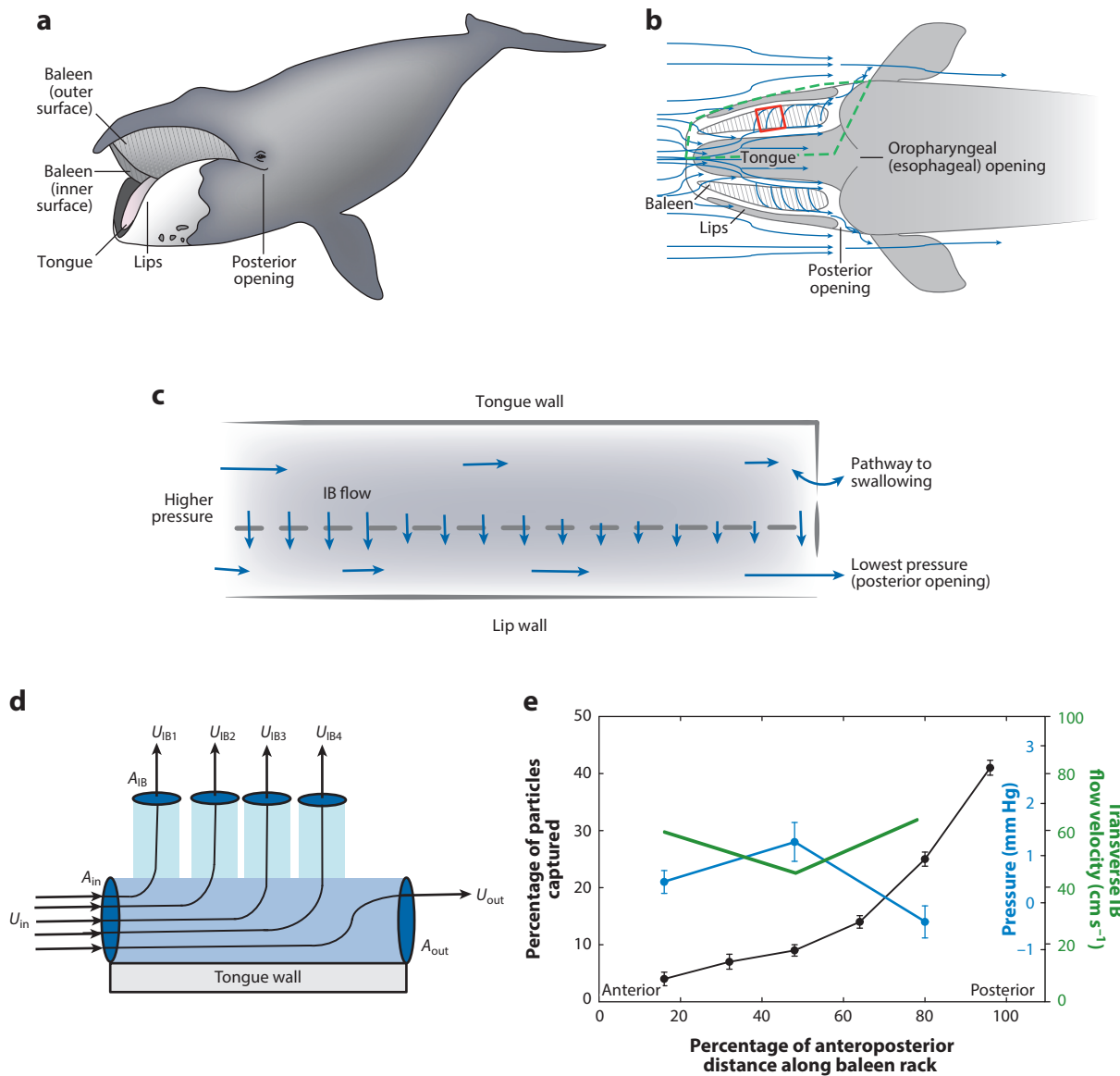
Aerial views of continuous ram filter feeding in bowhead whales and right whales (Balaenidae). (a) Oblique view. Photo by Dave Wiley. (b) Lateral view. Photo by Christin Khan (authorized by National Marine Fisheries Service permit #17355). (c) Dorsal view. Photo by John Durban, Holly Fearnbach, and Michael Moore [research approach of whales using unmanned aircraft systems (Durban et al. 2015) authorized by National Marine Fisheries Service permit #17355; flights authorized under Class G Memorandum of Understanding #2016-ESA-3-NOAA between the National Oceanic and Atmospheric Administration and the Federal Aviation Administration]. (d) Lateral view of multiple whales feeding in an echelon formation. Photo reproduced from Fish et al. (2013).

a drag that is correspondingly 100 times higher. This is clearly not a realistic foraging strategy. However, copepod densities of 0.01 kg m^{-3} and greater have been found in right and bowhead whale foraging hot spots (Baumgartner & Mate 2003), which suggests that the swimming speeds measured by Simon et al. (2009) are sufficient to meet basic energetic demands.

Although tagging studies have significantly increased our understanding of baleen whale foraging, they cannot yet elucidate the mechanisms that underlie the filtration process inside the mouth. However, laboratory studies have been used to infer hydrodynamic flow patterns and filtration processes. A recent study of the mechanical wear patterns on baleen plates and fringes provided new data on the directions and magnitudes of water flow during filtration (Werth et al. 2016). A subsequent study recreated the hypothesized fluid dynamics using flow tanks, specifically to assess the filtration performance of the baleen under simulated natural conditions (Werth &

Potvin 2016). Not only have flow tank experiments become critical for testing hypotheses about how baleen controls water flow through the mouth, but they have also suggested that the baleen can generate small lift forces (Werth & Potvin 2016) as well as Venturi forces (Werth 2004) that may decrease drag or negate compressive bow wave formation during ram feeding (Werth 2012).

Flow experiments and modeling refute the traditional view of the balaenid filter as analogous to the dead-end or throughput filter seen in many biological systems (Rubenstein & Koehl 1977). This type of filtration would involve water flow passing laterally between individual baleen plates from the inside to the outside of each baleen rack, where the direction of flow is largely perpendicular to the surface of the filter. Using flow tank experiments and hydrodynamic modeling of the balaenid engulfment apparatus, Werth & Potvin (2016) showed that cross-flow filtration



11.6 Goldbogen et al.

occurs, with most prey-laden water flowing parallel to (rather than perpendicularly through) the baleen filter, except at the posterior-most section of the filter, where prey accumulate for easier swallowing at the esophageal opening (**Figure 2**). An important consequence of cross-flow rather than throughput filtration is that it largely avoids clogging of the filter, precluding the need for periodic cleansing by mechanical scraping or hydrodynamic flushing (Werth 2001). Flow trials with and without simulated oral features such as the tongue and lips suggested that the primary agent of cross-flow generation is the hydrofoil-shaped baleen filter itself (Werth & Potvin 2016). Experimental recording of water flow speeds and pressures, along with kinematic analysis of buoyant particles flowing through the scaled, simulated balaenid mouth, yields strong evidence for cross-flow filtration, which has previously been documented in other filter-feeding vertebrates (Sanderson et al. 2001, 2016).

Balaenopteridae

In contrast to the continuous, low-speed, unidirectional ram filtration of bowhead and right whales, the rorquals (Balaenopteridae) exhibit a high-speed, intermittent, and sequential mechanism for filter feeding. The extraordinary engulfment capacity exhibited by rorqual whales during lunge feeding is enabled by an integrated and highly derived set of morphological adaptations (**Figure 3**). The engulfment apparatus consists of an elongated skull (Goldbogen et al. 2010, Pyenson et al. 2013), hyperextensible ventral groove blubber (VGB) that lines the oropharyngeal cavity (Orton & Brodie 1987, Shadwick et al. 2013), a tongue that is capable of inverting and expanding to accommodate the engulfed water (Lambertsen 1983), and a mechanosensory organ in the unfused mandibular symphysis (Pivorunas 1977, Pyenson et al. 2012). The kinematics of lunge feeding are highly dynamic (**Figures 4–8**), involving an acceleration to high speed and a subsequent deceleration (Goldbogen et al. 2006, Simon et al. 2012). During engulfment (**Figure 4**), the gape angle dynamics and rotation of the mandibles determine the area of the mouth exposed to flow and therefore the flux of water into the ventral pouch (Goldbogen et al. 2007, Potvin et al. 2009). The bowed mandibles of rorquals rotate outward during engulfment (Arnold et al. 2005, Lambertsen et al. 1995), a phenomenon that further enhances the area of the mouth exposed to the flow (**Figure 6**). Jaw rotation also applies to the lowering of the lower mandibles that coincides with the raising of the top of the skull (**Figures 4–6**). The simultaneous elevation of the skull and depression of the mandibles is thought to extend the magnitude of the gape angle and increase the torque capacity of the jaw-opening muscles (Koolstra & van Eijden 2004). Such a feature may be advantageous when rorquals experience extreme drag forces at high speed with a large projected mouth area

←

Figure 2

Engulfment and filtration mechanisms of bowhead whales and right whales (Balaenidae). (a) Schematic of balaenid functional anatomy. (b) Hypothesized flow patterns through and around the engulfment apparatus. The red box and green dashed line represent smaller flow fields studied by physical experiments and mathematical/computer modeling, respectively, in the study conducted by Werth & Potvin (2016). (c) Simplified dorsal view of one half of the cavity, showing the likely flow speeds and directions (Werth & Potvin 2016). The longest and shortest arrows correspond to the fastest and slowest speeds, respectively. The dashed line represents an array of ~300 fringed keratinous baleen plates suspended from the palate of balaenids. The double arrow on the right symbolizes the possibility of an open esophageal opening for engulfment of the filtered slurry. (d) Schematic view of the anteroposterior flows on the lingual and labial sides of the baleen rack, shown with lateral flows through baleen [intrabaleen (IB) flows]. Despite the drop of pressure longitudinally, the flows above the filter lose speed via mass loss through the lateral flows, per conservation of the mass rate; by contrast, longitudinal flows below the filter gain speed after merging with IB flows. This schematic diagram shows weakening axial flows via mass loss from IB flows through a cross filter (Werth & Potvin 2016). Per mass flow rate conservation, the exiting axial flow (U_{out}) becomes weaker after losing mass to IB filter surface outlets (of cross-section area $A_{\text{IB}i}$). (e) Pressure (blue line), flow speed (green line), and percentage of particles captured (black line) measured along the baleen rack. Figure modified from Werth & Potvin (2016).

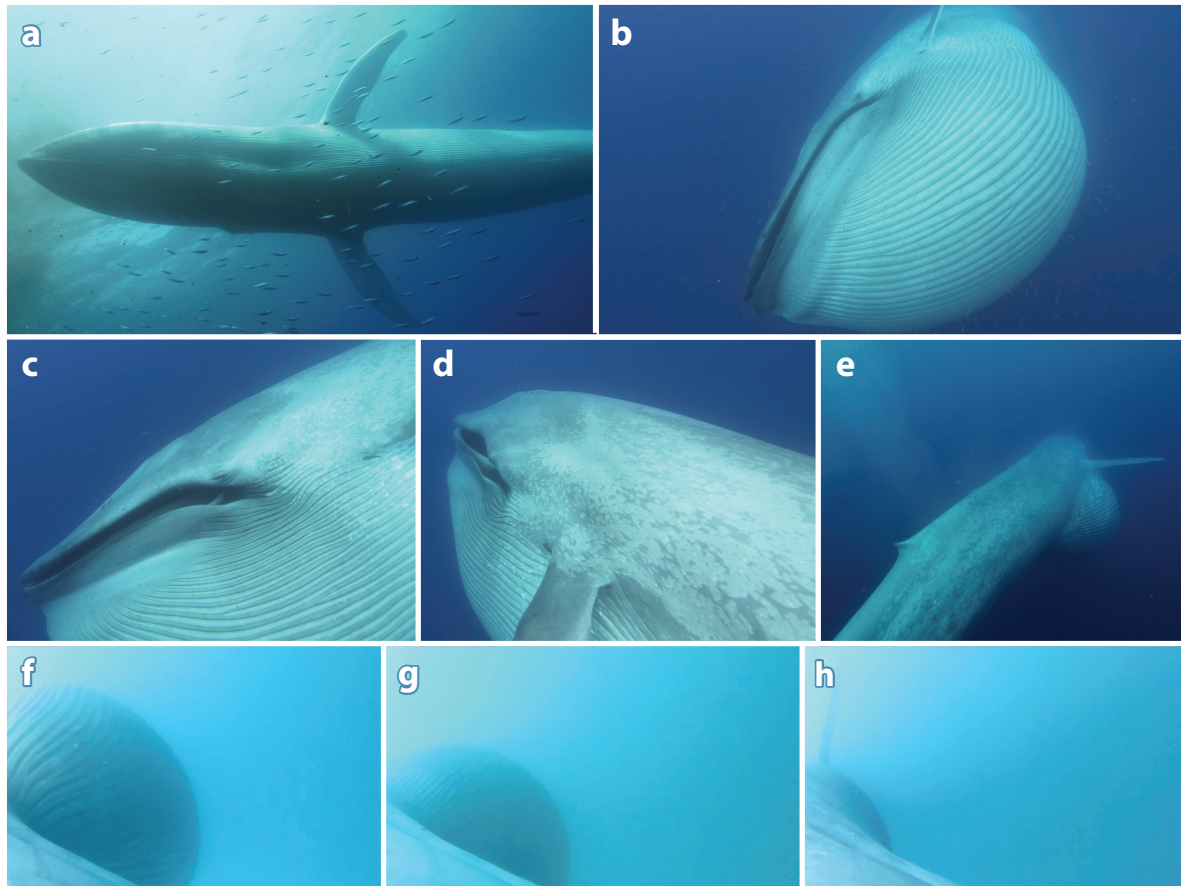


Figure 3

Underwater views of blue whale (*Balaenoptera musculus*) lunge filter feeding. (a) Ventral view of the ventral groove blubber, including a median ventral keel (Arnold et al. 2005). (b) Oblique view of the expanded ventral pouch, including the Y-shaped fibrocartilage skeleton that runs largely parallel to the mandibles (Pivorunas 1977). (c) Lateral view of the mouth slightly agape to expose the baleen, thereby facilitating filtration. (d) Oblique view of the mouth slightly agape, showing the outward rotation of the mandibles during filtration. (e) Oblique view of the expanded ventral pouch. (f–h) Posterior views of the ventral groove blubber and ventral pouch as it is compressed during the filtration and purging phases of engulfment. Panels a–e are from diver footage (authorized under National Marine Fisheries Service permit #16111) for the BBC program *The Hunt*, courtesy of Hugh Pearson; panels f–h are from whale-borne footage taken by a suction-cup-attached multisensor tag (authorized under National Marine Fisheries Service permit #16111).

(Goldbogen et al. 2007, Potvin et al. 2009). As dynamic pressure builds inside the ventral pouch, it drives the posteriorly directed expansion of the VGB (**Figure 5**). The capacitance of the ventral pouch is ultimately limited largely by the mechanical properties of the VGB, which is reversibly extensible up to several times its resting length (Orton & Brodie 1987).

From the mechanical properties of fin whale VGB and a simple cylindrical hydrostat model, Orton & Brodie (1987) originally hypothesized that a swimming speed of approximately 3 m s^{-1} would generate enough dynamic pressure to completely inflate the ventral pouch. In this engulfment scenario, termed passive engulfment, the inflation of the ventral pouch is resisted only by the elastic properties of VGB, with no impedance from muscle action. The first direct estimates of the maximum swimming speeds from lunge-feeding fin whales and quasi-steady hydrodynamic models

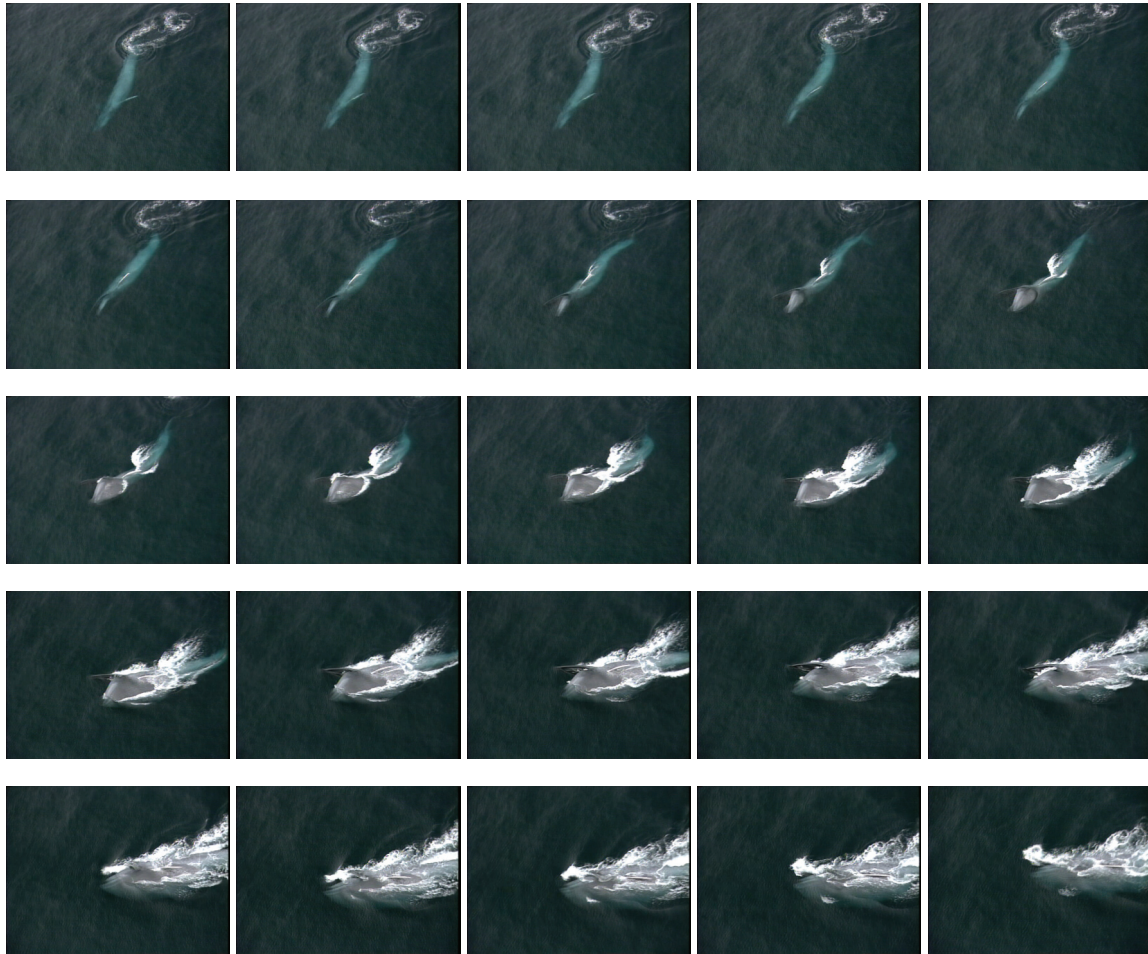


Figure 4

Aerial views of body kinematics during blue whale (*Balaenoptera musculus*) lunge filter feeding, showing the large degree of undulation along the body during engulfment. Images are from footage taken by Earl Richmond (authorized under National Marine Fisheries Service permit #16111), courtesy of Richmond Productions.

of engulfment, which were derived from flow noise measured using whale-borne tags, were largely consistent with this hypothesis (Goldbogen et al. 2006, 2007). However, a fundamental flaw of these studies was that they failed to account for the acceleration of engulfed water from inside the ventral pouch, a process that would be required when a moving whale engulfs a volume of water that is initially at rest. Unsteady hydromechanical models of engulfment suggested that the passive engulfment mechanism may not be feasible primarily because it does not generate enough VGB force onto the engulfed mass to account for the large and rapid deceleration observed following maximum lunge speed (Potvin et al. 2009). Moreover, the passive engulfment scenario resulted in the ventral pouch reaching maximum capacity in much less time than observed in vivo, in large part because of a lack of resistance to the rapidly expanding VGB (Potvin et al. 2009).

Based on these simulations, researchers hypothesized a different engulfment mechanism called active engulfment, in which eccentric muscle action dynamically resists the inflation of VGB

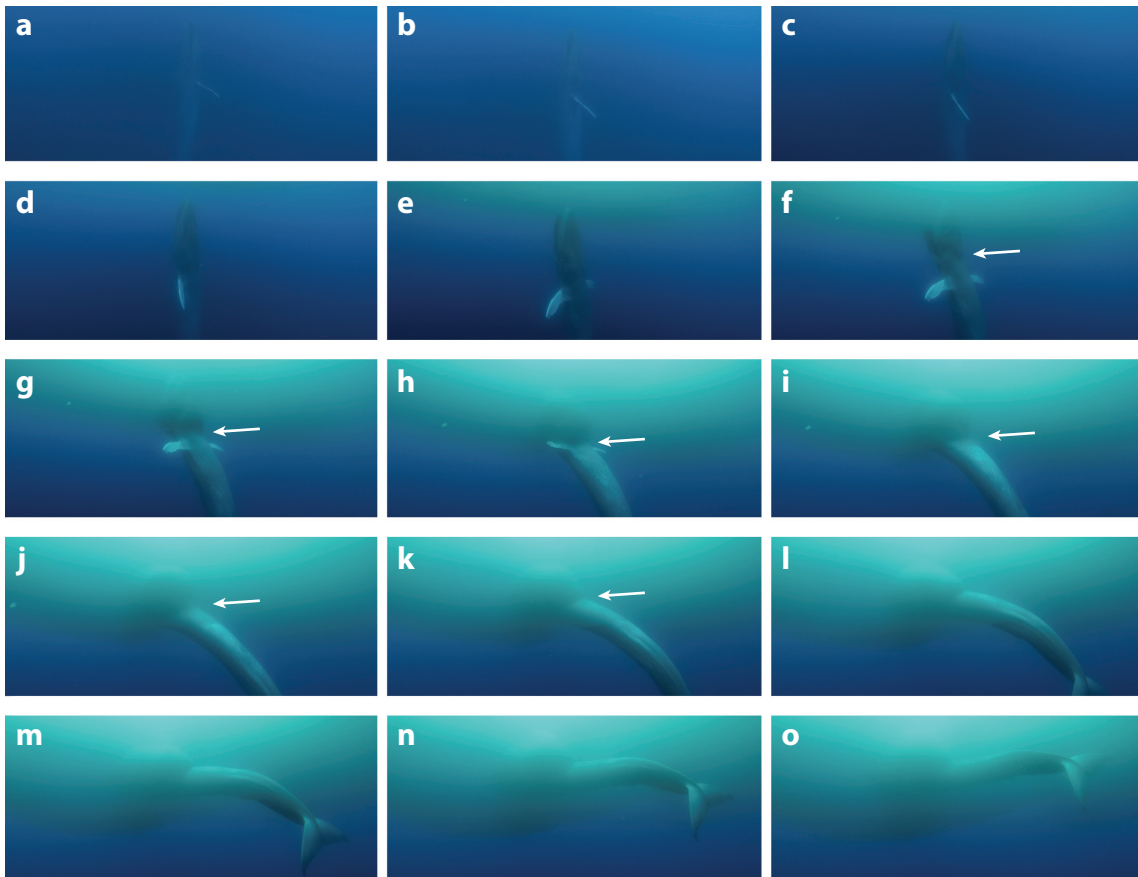


Figure 5

Underwater views of the engulfment phase of blue whale (*Balaenoptera musculus*) lunge filter feeding. (*a–e*) Prey approach ascent (panels *a–c*) is followed by mouth opening (panels *d* and *e*), which reveals an intermandibular depression of the floor of the mouth and ventral groove blubber. (*f–o*) Dynamic pressure builds within the oropharyngeal cavity and expands the ventral groove blubber in a posteriorly propagating wave (*arrows*). Images are from diver footage (authorized under National Marine Fisheries Service permit #16111) for the BBC program *The Hunt*, courtesy of Hugh Pearson.

(Potvin et al. 2009). By action-reaction, the combined elastic and muscular forces accelerate the water and the suspended prey being engulfed (Potvin et al. 2009). As the whale transfers its momentum to the engulfed water mass, the whale decelerates but the engulfed water mass continues to accelerate, with the latter contributing an additional source of drag called engulfment drag. These models suggest that, at the end of engulfment, the speed of the decelerated whale is similar to that of the accelerated water (Goldbogen et al. 2011, Potvin et al. 2012). In simulation, engulfment drag is added to typical bluff body shape drag from the flow around the body, yielding deceleration signatures similar to those in empirical data (Goldbogen et al. 2011, Potvin et al. 2009). Eccentric muscle action from the VGB musculature may also be required to prevent pouch extensions that are beyond the known physiological limits of vertebrate muscle (Shadwick et al. 2013).

Recent histological and morphometric analyses of VGB suggest that the ventral pouch expansion (or strain) during engulfment is less than previously thought (Shadwick et al. 2013). The maximal circumferential extensions were estimated as 160% of the resting VGB length

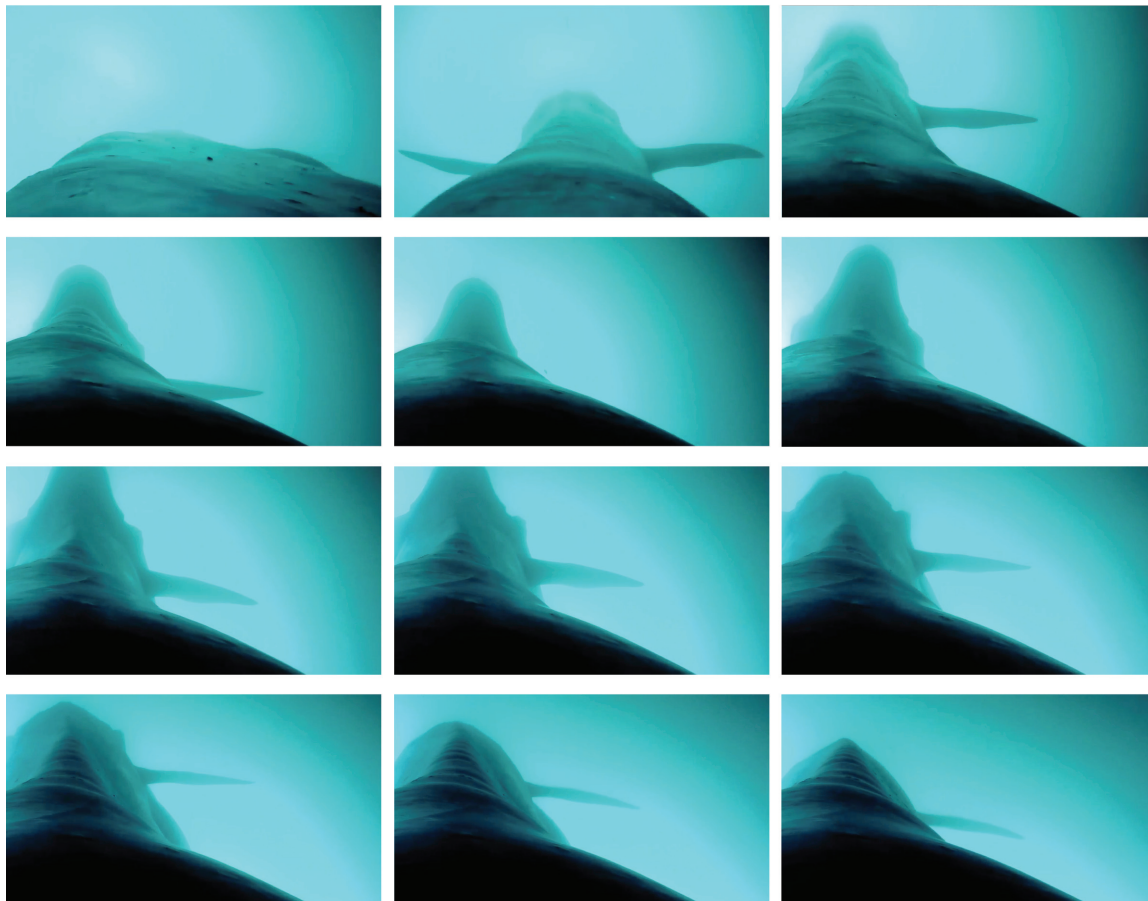


Figure 6

Whale-borne multisensor-tag views of the engulphment phase of blue whale (*Balaenoptera musculus*) lunge filter feeding. The engulphment phase from mouth opening to mouth closure is marked by the elevation and lowering of the rostrum, respectively. The outward and inward rotation of the lower mandibles is also evident. Images are from whale-borne footage taken by a suction-cup-attached multisensor tag (authorized under National Marine Fisheries Service permit #16111).

(Shadwick et al. 2013), rather than the 400% observed during mechanical tests in which the VGB was stretched to its elastic limit (Orton & Brodie 1987). Even if the VGB were stretched less than the elastic limit, the high strains represent a major mechanical challenge for the muscles associated with the VGB (Shadwick et al. 2013). Moreover, smaller maximal strains suggest that the amount of VGB elastic (mechanical) energy—63 kJ, as estimated at 160% strain from the stress-strain data of Orton & Brodie (1987)—is insufficient to account for the 125 kJ of kinetic energy lost by the masses of the whale and engulfed water when decelerating from 3.0 m s^{-1} to approximately 1.0 m s^{-1} while lunging on krill (Goldbogen et al. 2006, Potvin et al. 2009). However, histological evidence demonstrates that the VGB muscles exhibit a folded microstructure, which enables the muscles to unfold during VGB expansion and still remain operational within the known strain limits of skeletal muscle (Shadwick et al. 2013). The eccentric activity of the VGB muscles may be used to resist the expansion of the ventral pouch during lunge feeding, which could explain the common observation of VGB strains that are lower than the elastic limit (Shadwick et al.

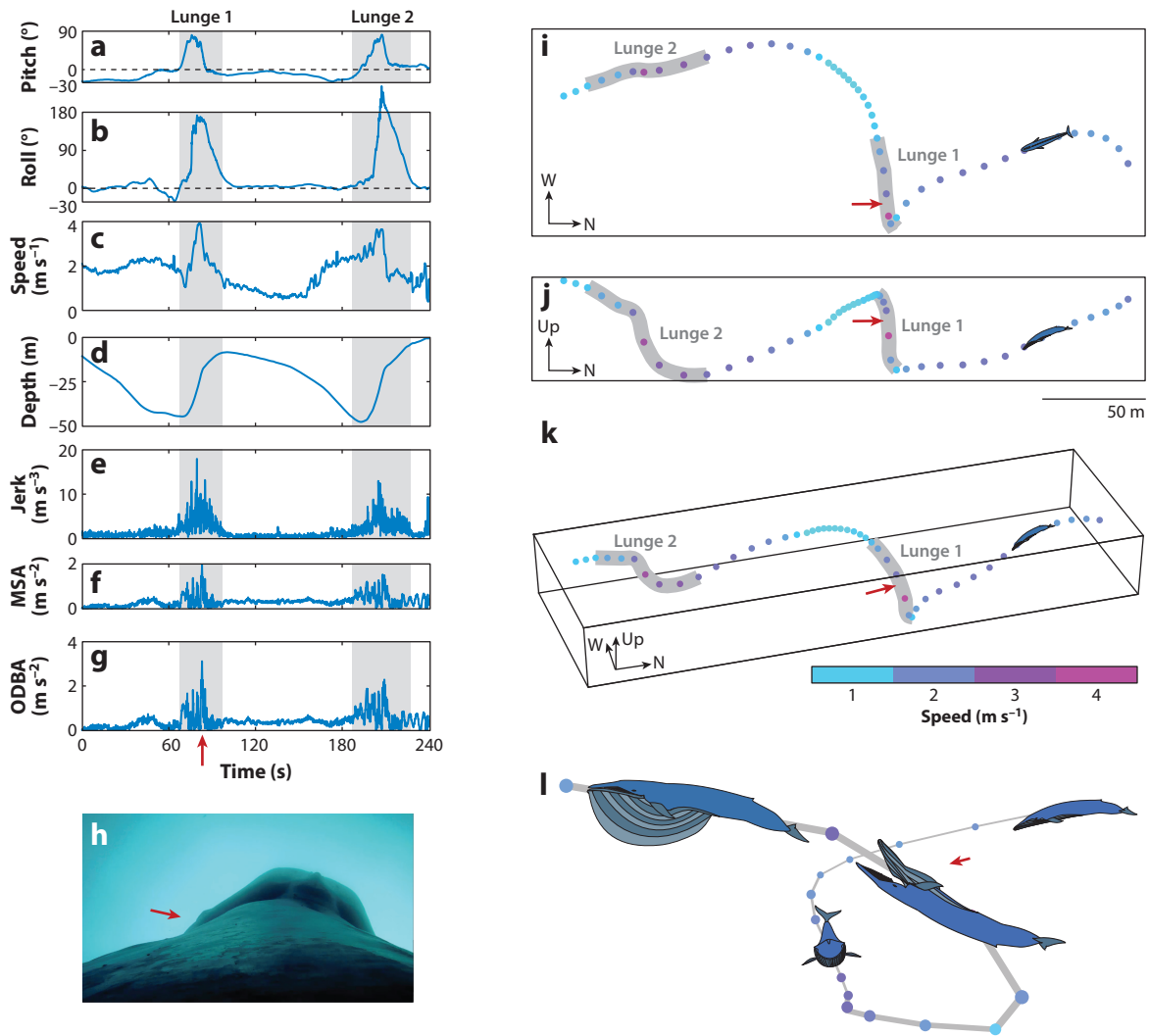


Figure 7

Body kinematics during blue whale (*Balaenoptera musculus*) lunge filter feeding. (a–g) The kinematic patterns of two lunges, showing (a) pitch, (b) roll, (c) speed, (d) depth, (e) jerk (or rate of acceleration), (f) minimum specific acceleration (MSA), and (g) overall dynamic body acceleration (ODBA). (h) An image from whale-borne footage taken by a suction-cup-attached multisensor tag (authorized under National Marine Fisheries Service permit #16111), showing the timing of the mouth opening during the first lunge (red arrows). (i–k) The trajectory of the whale shown (i) from above, (j) from the side, and (k) in three dimensions. (l) A reconstructed view of the first feeding lunge, showing the acrobatic upward roll used by the whale.

2013). Perhaps this is a way that rorquals can modulate the size of the engulfed water mass when maximum engulfment capacity is not needed (i.e., when feeding on smaller prey patches).

Although the hypothesized active engulfment mechanism appears to account for several phenomena associated with the dynamics of lunge feeding in large rorquals, we predict that it may not be universal under all scenarios and across all scales. Considering the importance of scale in determining the mechanics and performance of lunge feeding (Goldbogen et al. 2010, 2012; Potvin et al. 2010, 2012), we suspect that the elastic potential energy within the VGB could be a

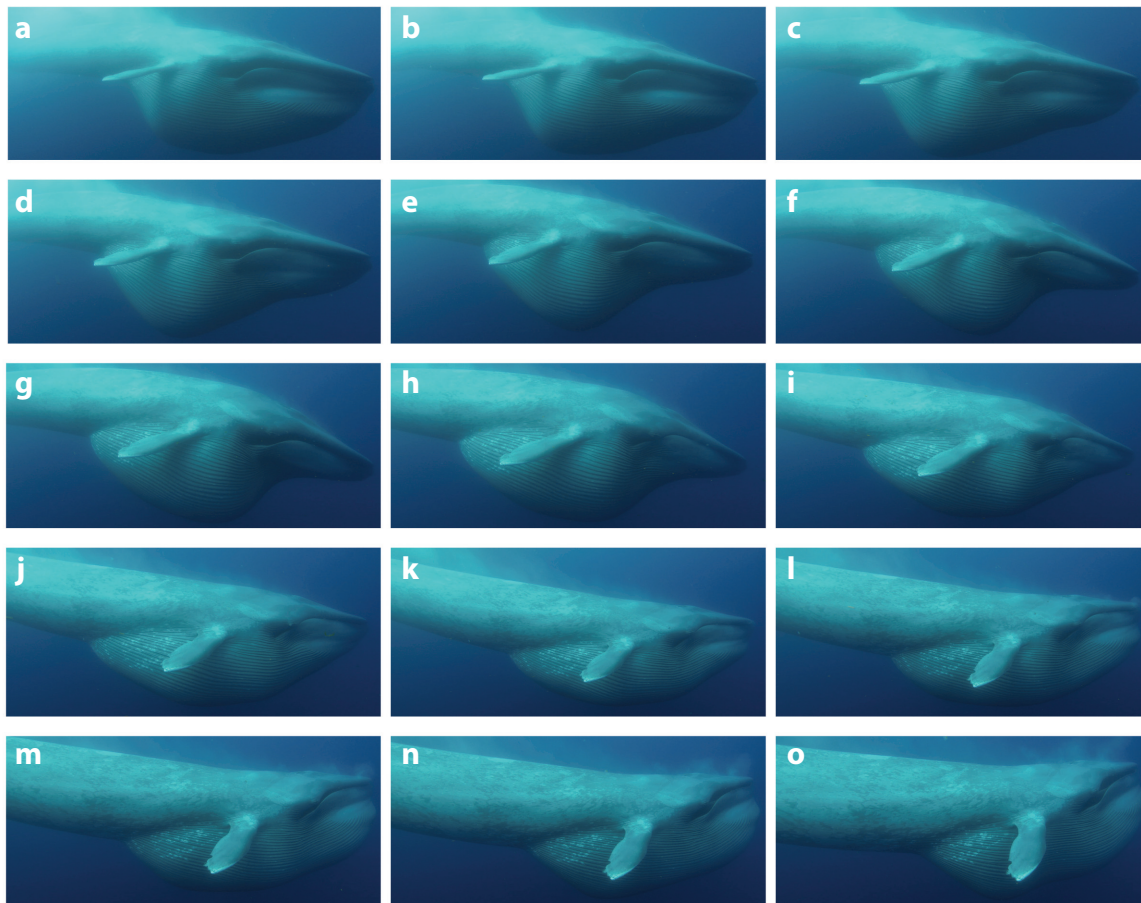


Figure 8

Underwater views of the filtration phase of blue whale (*Balaenoptera musculus*) lunge filter feeding. After the mouth closes around a large volume of prey-laden water, the expanded ventral pouch contracts to force water past the baleen and out of the mouth. Muscles within the ventral groove blubber are thought to power the purging of the ventral pouch. Here, the whale actively pushes engulfed water first posteriorly (panels *a–f*) and then anteriorly (panels *g–l*), which is followed by the outer rotation of the lower mandibles to increase the area of baleen being used in filtration (panels *m–o*). Images are from diver footage (authorized under National Marine Fisheries Service permit #16111) for the BBC program *The Hunt*, courtesy of Hugh Pearson.

significant driver of the engulfment process in a more passive mechanism in smaller rorquals such as minke whales (*Balaenoptera acutorostrata*). Because minke whales occupy the lower body size range for lunge feeders, their mass-specific engulfment capacity (engulfment capacity relative to body mass) is lower than that of larger rorqual species (Friedlaender et al. 2014). This is due largely to the allometry of the engulfment apparatus, with larger rorquals exhibiting relatively larger skulls and buccal cavities (Goldbogen et al. 2010, 2012). The low mass-specific engulfment capacity in small rorquals suggests that the momentum transfer from the whale to the engulfed water should also be less, and as a result, smaller rorquals should be able to retain more momentum during lunge feeding. Indeed, tag studies have shown that humpback whales exhibit higher speeds after engulfment compared with larger species (Simon et al. 2012), including fin whales (Goldbogen et al. 2006) and blue whales (Goldbogen et al. 2011), which may represent the different relative

scales of momentum transfer from whale to water. Whether engulfment is fully active, passive, or a combination of both will crucially depend on body size and on how much of the pouch is being filled under the active control of the VGB muscles. One way these hypotheses could be tested more rigorously is by analyzing the kinematics of the body and skull as well as the strain rate of VGB expansion, especially with respect to the timing of the deceleration phase relative to the engulfment phase. Such an approach would require integrated video and movement sensors in whale-borne tags.

The water flow patterns inside the mouth during rorqual filtration and purging remain poorly understood. The potential for an active engulfment mechanism, and the acceleration of engulfed water, suggests that the water inside the mouth may be in motion after the mouth closure.

This acceleration of engulfed water inside the ventral pouch may facilitate the purported cross-flow filtration mechanism after mouth closure (Potvin et al. 2009). Cross-flow filtration was first hypothesized as a potential mechanism in rorquals after initial estimates of the speeds and Reynolds numbers of flow past baleen fringes were found to be similar to those in suspension filter-feeding fishes that use cross-flow (Goldbogen et al. 2007). Given that the ventral pouch is well muscularized, it is possible that rorquals can actively move engulfed water back and forth inside the pouch to further enhance cross-flow filtration (**Figure 8**). Although recent experimental and modeling studies suggest that cross-flow filtration is the most likely mechanism used by balaenid whales (Werth & Potvin 2016), the rorqual filtration process is virtually unknown, and further study is critically needed.

Hydrodynamic modeling provided an additional important insight into the mechanics of engulfment: Complete inflation is possible at maximum lunge speeds that are much lower than those estimated from tag data (Goldbogen et al. 2012). Such a strategy would yield lower energetic costs because both engulfment drag and shape drag are influenced by the square of the swimming speed. However, this may not be optimal with respect to prey capture (Potvin et al. 2010), especially for prey with well-developed escape responses (Domenici 2001, O'Brien 1987). As a result, rorquals must increase maximum lunge speeds to efficiently capture prey during engulfment, but at the cost of greater energy expenditure (Potvin et al. 2012). Comparative tag data for three rorqual species (blue whales, fin whales, and humpback whales) feeding on the same prey type (krill in the eastern North Pacific) support this hypothesis by demonstrating larger maximum lunge speeds in progressively larger rorqual species (Goldbogen et al. 2012). Larger rorquals should be detected by prey at a greater distance, which would induce the early onset of prey escape maneuvers (Domenici 2002, O'Brien 1987), thus requiring higher attack speeds by the whales to overcome the escape speed of prey (Goldbogen et al. 2012). Furthermore, the maneuverability of the predator relative to prey is diminished with increasing predator-prey body size ratios (Domenici 2001), which would also theoretically decrease prey capture efficiency at a given level of predator attack performance. Predators may be able to avoid early visual detection by attacking prey from below (Goldbogen et al. 2013a) or along axes of sunlight for concealment (Huvneers et al. 2015), thereby minimizing prey escape responses and maximizing prey capture and foraging efficiency.

FOUR OUTSTANDING BIG-PICTURE QUESTIONS IN BALEEN WHALE FORAGING

Despite several major recent advances in our understanding of how whales feed, much more research is needed to address even the most basic questions in this logistically challenging field of study. Here, we outline the most significant big-picture questions that remain untested and deserve future research effort. Many of these questions span multiple disciplines and require integrative approaches at the interface of physiology, biomechanics, and foraging ecology.

How Do Baleen Whales Find Prey at Different Temporal and Spatial Scales?

Many baleen whale species feed on dynamic, seasonally abundant, and ephemeral prey (Croll et al. 2005, Wiedenmann et al. 2011). A major gap in our understanding of this predator-prey dynamic relates to how baleen whales locate food—and, specifically, what abiotic or biotic environmental cues whales use to home in on these patchy resources. This is critically important because baleen whales require high-density prey for efficient foraging, so these predators cannot rely on sparsely distributed food (Goldbogen et al. 2011).

This problem has multiple temporal and spatial components that are nested in a hierarchical manner (Benoit-Bird et al. 2013). First, mysticetes must locate specific habitats within large oceanic ecosystems that offer the necessary components (e.g., light and nutrients) to promote primary and secondary productivity. Second, baleen whales not only must find discrete patches of prey within the environment, but also must target the densest parts of these patches for optimal efficiency, a challenge that could vary on a dive-by-dive or even a foraging bout-by-bout basis. Therefore, whales are faced with the problem of food localization in three spatial dimensions, where the abundance and distribution of food will vary dramatically as a function of time. The sensory modes used to find prey are completely unknown, and whales may use unique combinations of modes depending on the ecological scale and context.

How Do Baleen Whales Optimize Foraging Efficiency in Patchily Distributed, Heterogeneous Prey Fields?

Because food resources vary significantly through space and time, whales must modulate their feeding rates and foraging strategies to optimize energetic efficiency. Baleen whales are air-breathing divers, and therefore their foraging performance is ultimately constrained by a combination of oxygen supply, rate of oxygen use, and hypoxemic tolerance. However, high-quality (dense) prey patches often occur at depth relative to less dense patches, which tend to be shallower (Friedlaender et al. 2016, Goldbogen et al. 2015a, Hazen et al. 2015). Diving whales can increase their dive duration and feeding rates to maximize energy gain, but this comes at the expense of increased oxygen debt, which requires extended postdive recovery time at the sea surface following foraging dives (Acevedo-Gutiérrez et al. 2002). Therefore, whales must optimize two competing processes (Hazen et al. 2015): minimizing oxygen use during diving and maximizing energy intake from feeding. Although studies have demonstrated that baleen whales optimize both key energetic currencies across prey density and depth gradients (Friedlaender et al. 2013, Goldbogen et al. 2008, Hazen et al. 2015), it is unclear how optimal foraging strategies vary within a species when feeding on different prey. Moreover, it is virtually unknown how optimal foraging behavior should vary across different-sized predators that feed on similar prey, where mechanical scaling effects are expected to play a major role in constraining foraging performance (Goldbogen et al. 2012).

How Does the Scaling of Maneuvering Performance Limit Foraging in Baleen Whales?

Larger animals generally exhibit decreased maneuvering capacity compared with smaller animals (Domenici 2001, Webb & De Buffrénil 1990). Because large whales feed on animals that are smaller by several orders of magnitude, this presents a major challenge for efficient prey capture (Domenici 2001). As a result, large whales have evolved behavioral strategies (e.g., bubble-net feeding and tail slapping) and foraging mechanisms (filter feeding) that effectively minimize the importance of

this difference in unsteady locomotor capacity (Domenici 2001, Domenici et al. 2000, Goldbogen et al. 2013a, Webb & De Buffrénil 1990, Wiley et al. 2011). What remains unknown is how maneuvering capacity scales across taxa in baleen whales. If maneuverability is diminished in larger body sizes, it may constrain foraging performance and thus may have influenced the evolution of prey preferences (Goldbogen et al. 2010, 2013a, 2015a) and the structure of pelagic communities.

What Are the Biomechanical Mechanisms of Engulfment and Filtration in Baleen Whales?

Despite major technological advances and a wide range of integrative studies, we still do not fully understand all of the functional mechanisms that underlie foraging in baleen whales. Future research should focus on two complementary pathways to obtain new information: biologging and experimental flow tank studies. The biologging of kinematic parameters is a powerful approach that will become increasingly effective with the ever-evolving sensing capacity of animal-borne instrumentation. For rorquals in particular, simultaneous kinematic data of the skull, body, and expanding VGB during lunge feeding will allow us to test competing hypotheses that describe the engulfment mechanism. The baleen filtration mechanism is becoming more understood, but we still do not know how the differences in baleen morphology affect hydrodynamic flow and filtration performance for the efficient capture and processing of different prey types. There is a tremendous diversity in rorqual baleen anatomy, but few studies have addressed its functional and ecological consequences.

DISCLOSURE STATEMENT

The authors are not aware of any affiliations, memberships, funding, or financial holdings that might be perceived as affecting the objectivity of this review.

ACKNOWLEDGMENTS

We thank Customized Animal Telemetry Solutions for their assistance with manufacturing dual-lens cameras and 3-D movement tags. Images were obtained for scientific research under National Marine Fisheries Service permit #16111 (J. Calambokidis) in collaboration with Hugh Pearson, David Reichert, Silverback Films, and the BBC. We also thank members of the Cascadia Research Collective, including Jeff Foster and James Fahlbusch, for their assistance with tagging and boat operations.

LITERATURE CITED

- Acevedo-Gutiérrez A, Croll DA, Tershy BR. 2002. High feeding costs limit dive time in the largest whales. *J. Exp. Biol.* 205:1747–53
- Alexander RM. 1998. All-time giants: the largest animals and their problems. *Palaeontology* 41:1231–45
- Aoki K, Amano M, Mori K, Kourogi A, Kubodera T, Miyazaki N. 2012. Active hunting by deep-diving sperm whales: 3D dive profiles and maneuvers during bursts of speed. *Mar. Ecol. Prog. Ser.* 444:289–301
- Arnold PW, Birtles RA, Soltzick S, Matthews M, Dunstan A. 2005. Gulping behaviour in rorqual whales: underwater observations and functional interpretation. *Mem. Queensl. Mus.* 51:309–32
- Baumgartner MF, Cole TVN, Campbell RG, Teegarden GJ, Durbin EG. 2003. Associations between North Atlantic right whales and their prey, *Calanus finmarchicus*, over diel and tidal time scales. *Mar. Ecol. Prog. Ser.* 264:155–66

- Baumgartner MF, Mate BR. 2003. Summertime foraging ecology of North Atlantic right whales. *Mar. Ecol. Prog. Ser.* 264:123–35
- Benoit-Bird KJ, Battaile BC, Nordstrom CA, Trites AW. 2013. Foraging behavior of northern fur seals closely matches the hierarchical patch scales of prey. *Mar. Ecol. Prog. Ser.* 479:283–302
- Bloodworth B, Marshall CD. 2005. Feeding kinematics of *Kogia* and *Tursiops* (Odontoceti: Cetacea): characterization of suction and ram feeding. *J. Exp. Biol.* 208:3721–30
- Brodie PF. 1975. Cetacean energetics, an overview of intraspecific size variation. *Ecology* 56:152–61
- Charnov EL. 1976. Optimal foraging, the marginal value theorem. *Theor. Popul. Biol.* 9:129–36
- Croll DA, Marinovic B, Benson S, Chavez FP, Black N, et al. 2005. From wind to whales: trophic links in a coastal upwelling system. *Mar. Ecol. Prog. Ser.* 289:117–30
- Demere TA, McGowen MR, Berta A, Gatesy J. 2008. Morphological and molecular evidence for a stepwise evolutionary transition from teeth to baleen in mysticete whales. *Syst. Biol.* 57:15–37
- Domenici P. 2001. The scaling of locomotor performance in predator-prey encounters: from fish to killer whales. *Comp. Biochem. Physiol. A* 131:169–82
- Domenici P. 2002. The visually mediated escape response in fish: predicting prey responsiveness and the locomotor behaviour of predators and prey. *Mar. Freshw. Behav. Physiol.* 35:87–110
- Domenici P, Batty RS, Simila T, Ogam E. 2000. Killer whales (*Orcinus orca*) feeding on schooling herring (*Clupea harengus*) using under-water tail-slaps: kinematic analyses of field observations. *J. Exp. Biol.* 203:283–94
- Durban J, Fearnbach H, Barrett-Lennard L, Perryman W, Leroi D. 2015. Photogrammetry of killer whales using a small hexacopter launched at sea 1. *J. Unmanned Veh. Syst.* 3:131–35
- Ekdale EG, Deméré TA, Berta A. 2015. Vascularization of the gray whale palate (Cetacea, Mysticeti, *Eschrichtius robustus*): soft tissue evidence for an alveolar source of blood to baleen. *Anat. Rec.* 298:691–702
- Eschricht DF, Reinhardt JT. 1866. On the Greenland right whale (*Balaena mysticetus* Linn.) with especial reference to its geographical distribution and migrations in times past and present, and to its external and internal characteristics. In *Recent Memoirs on the Cetacea by Professors Eschricht, Reinhardt, and Lilljeborg*, ed. WH Flower, pp. 1–150. London: Ray Soc.
- Fish FE, Goetz KT, Rugh DJ, Brattström LV. 2013. Hydrodynamic patterns associated with echelon formation swimming by feeding bowhead whales (*Balaena mysticetus*). *Mar. Mamm. Sci.* 29:E498–507
- Fitzgerald EMG. 2006. A bizarre new toothed mysticete (Cetacea) from Australia and the early evolution of baleen whales. *Proc. R. Soc. Lond. B* 273:2955–63
- Fitzgerald EMG. 2012. Archaeocete-like jaws in a baleen whale. *Biol. Lett.* 8:94–96
- Ford TJ, Werth AJ, George JC. 2013. An intraoral thermoregulatory organ in the bowhead whale (*Balaena mysticetus*), the corpus cavernosum maxillaris. *Anat. Rec.* 296:701–8
- Fordyce RE, Marx FG. 2013. The pygmy right whale *Caperea marginata*: the last of the cetotheres. *Proc. R. Soc. Lond. B* 280:20122645
- Friedlaender AS, Goldbogen JA, Nowacek DP, Read AJ, Johnston D, Gales N. 2014. Feeding rates and under-ice foraging strategies of the smallest lunge filter feeder, the Antarctic minke whale (*Balaenoptera bonaerensis*). *J. Exp. Biol.* 217:2851–54
- Friedlaender AS, Hazen EL, Goldbogen JA, Stimpert AK, Calambokidis J, Southall BL. 2016. Prey-mediated behavioral responses of feeding blue whales in controlled sound exposure experiments. *Ecol. Appl.* 26:1075–85
- Friedlaender AS, Hazen EL, Nowacek DP, Halpin PN, Ware C, et al. 2009. Diel changes in humpback whale *Megaptera novaeangliae* feeding behavior in response to sand lance *Ammodytes* spp. behavior and distribution. *Mar. Ecol. Prog. Ser.* 395:91–100
- Friedlaender AS, Tyson RB, Stimpert AK, Read AJ, Nowacek DP. 2013. Extreme diel variation in the feeding behavior of humpback whales along the western Antarctic Peninsula during autumn. *Mar. Ecol. Prog. Ser.* 494:281–89
- Fudge DS, Szewciw LJ, Schwalb AN. 2009. Morphology and development of blue whale baleen: an annotated translation of Tycho Tullberg's classic 1883 paper. *Aquat. Mamm.* 35:226–52
- Goldbogen JA. 2010. The ultimate mouthful: lunge feeding in rorqual whales. *Am. Sci.* 98:124–31
- Goldbogen JA, Calambokidis J, Croll DA, Harvey JT, Newton KM, et al. 2008. Foraging behavior of humpback whales: kinematic and respiratory patterns suggest a high cost for a lunge. *J. Exp. Biol.* 211:3712–19

- Goldbogen JA, Calambokidis J, Croll DA, McKenna MF, Potvin J, et al. 2012. Scaling of lunge feeding performance in rorqual whales: mass-specific energy expenditure increases with body size and progressively limits diving capacity. *Funct. Ecol.* 26:216–26
- Goldbogen JA, Calambokidis J, Friedlaender AS, Francis J, DeRuiter SL, et al. 2013a. Underwater acrobatics by the world's largest predator: 360 degrees rolling manoeuvres by lunge-feeding blue whales. *Biol. Lett.* 9:20120986
- Goldbogen JA, Calambokidis J, Oleson E, Potvin J, Pyenson ND, et al. 2011. Mechanics, hydrodynamics and energetics of blue whale lunge feeding: efficiency dependence on krill density. *J. Exp. Biol.* 214:131–46
- Goldbogen JA, Calambokidis J, Shadwick RE, Oleson EM, McDonald MA, Hildebrand JA. 2006. Kinematics of foraging dives and lunge-feeding in fin whales. *J. Exp. Biol.* 209:1231–44
- Goldbogen JA, Friedlaender AS, Calambokidis J, McKenna MF, Simon M, Nowacek DP. 2013b. Integrative approaches to the study of baleen whale diving behavior, feeding performance, and foraging ecology. *BioScience* 63:90–100
- Goldbogen JA, Hazen EL, Friedlaender AS, Calambokidis J, DeRuiter SL, et al. 2015a. Prey density and distribution drive the three-dimensional foraging strategies of the largest filter feeder. *Funct. Ecol.* 29:951–61
- Goldbogen JA, Meir JU. 2014. The device that revolutionized marine organismal biology. *J. Exp. Biol.* 217:167–68
- Goldbogen JA, Potvin J, Shadwick RE. 2010. Skull and buccal cavity allometry increase mass-specific engulfment capacity in fin whales. *Proc. R. Soc. B* 277:861–68
- Goldbogen JA, Pyenson ND, Shadwick RE. 2007. Big gulps require high drag for fin whale lunge feeding. *Mar. Ecol. Prog. Ser.* 349:289–301
- Goldbogen JA, Shadwick RE, Lillie MA, Piscitelli MA, Potvin J, et al. 2015b. Using morphology to infer physiology: case studies on rorqual whales (Balaenopteridae) 1. *Can. J. Zool.* 93:687–700
- Hazen EL, Friedlaender AS, Goldbogen JA. 2015. Blue whales (*Balaenoptera musculus*) optimize foraging efficiency by balancing oxygen use and energy gain as a function of prey density. *Sci. Adv.* 1:e1500469
- Hazen EL, Friedlaender AS, Thompson MA, Ware CR, Weinrich MT, et al. 2009. Fine-scale prey aggregations and foraging ecology of humpback whales *Megaptera novaeangliae*. *Mar. Ecol. Prog. Ser.* 395:75–89
- Huveneers C, Holman D, Robbins R, Fox A, Endler JA, Taylor AH. 2015. White sharks exploit the sun during predatory approaches. *Am. Nat.* 185:562–70
- Johnson KR, Nelson CH. 1984. Side-scan sonar assessment of gray whale feeding in the Bering Sea. *Science* 225:1150–52
- Johnson M, Tyack PL. 2003. A digital acoustic recording tag for measuring the response of wild marine mammals to sound. *IEEE J. Ocean. Eng.* 28:3–12
- Kane EA, Marshall CD. 2009. Comparative feeding kinematics and performance of odontocetes: belugas, Pacific white-sided dolphins and long-finned pilot whales. *J. Exp. Biol.* 212:3939–50
- Koolstra JH, van Eijden T. 2004. Functional significance of the coupling between head and jaw movements. *J. Biomech.* 37:1387–92
- Krogh A. 1929. The progress of physiology. *Am. J. Physiol.* 90:243–51
- Laidre KL, Heide-Jørgensen MP, Nielsen TG. 2007. Role of the bowhead whale as a predator in West Greenland. *Mar. Ecol. Prog. Ser.* 346:285–97
- Lambertsen RH. 1983. Internal mechanism of rorqual feeding. *J. Mamm.* 64:76–88
- Lambertsen RH, Rasmussen KJ, Lancaster WC, Hintz RJ. 2005. Functional morphology of the mouth of the bowhead whale and its implications for conservation. *J. Mamm.* 86:342–52
- Lambertsen RH, Ulrich N, Straley J. 1995. Frontomandibular stay of Balaenopteridae: a mechanism for momentum recapture during feeding. *J. Mamm.* 76:877–99
- Lindberg DR, Pyenson ND, Estes JA, Demaster DP, Doak DF, et al. 2006. Evolutionary patterns in Cetacea: fishing up prey size through deep time. In *Whales, Whaling, and Ocean Ecosystems*, ed. ed. JA Estes, DP DeMaster, DF Doak, TM Williams, RL Brownell, pp. 67–81. Berkeley: Univ. Calif. Press
- Lockyer CH. 1976. Body weights of some species of large whales. *ICES J. Mar. Sci.* 36:259–73
- Lockyer CH. 1981. Growth and energy budgets of large baleen whales from the Southern Hemisphere. In *Mammals in the Seas, Vol. 3: General Papers and Large Cetaceans*, ed. JG Clark, pp. 379–487. Rome: Food Agric. Organ. UN

- Madsen PT, de Soto NA, Arranz P, Johnson M. 2013. Echolocation in Blainville's beaked whales (*Mesoplodon densirostris*). *J. Comp. Physiol. A* 199:451–69
- Miller PJO, Johnson MP, Tyack PL. 2004. Sperm whale behaviour indicates the use of echolocation click buzzes 'creaks' in prey capture. *Proc. R. Soc. Lond. B* 271:2239–47
- Mori Y. 1998. Optimal choice of foraging depth in divers. *J. Zool.* 245:279–83
- Mori Y. 2002. Optimal diving behaviour for foraging in relation to body size. *J. Evol. Biol.* 15:269–76
- Motta PJ, Maslanka M, Hueter RE, Davis RL, de la Parra R, et al. 2010. Feeding anatomy, filter-feeding rate, and diet of whale sharks *Rhincodon typus* during surface ram filter feeding off the Yucatan Peninsula, Mexico. *Zoology* 113:199–212
- Nerini M. 1984. A review of gray whale feeding ecology. In *The Gray Whale: Eschrichtius robustus*, ed. ML Jones, SL Swartz, S Leatherwood, pp. 423–50. Orlando, FL: Academic
- Nousek-McGregor AE. 2010. *The cost of locomotion in North Atlantic right whales Eubalaena glacialis*. PhD Thesis, Duke Univ., Durham, NC
- O'Brien DP. 1987. Description of escape responses of krill (Crustacea, Euphausiacea), with particular reference to swarming behavior and the size and proximity of the predator. *J. Crustac. Biol.* 7:449–57
- Orton LS, Brodie PF. 1987. Engulfing mechanics of fin whales. *Can. J. Zool.* 65:2898–907
- Paig-Tran EM, Bizzarro JJ, Strother JA, Summers AP. 2011. Bottles as models: predicting the effects of varying swimming speed and morphology on size selectivity and filtering efficiency in fishes. *J. Exp. Biol.* 214:1643–54
- Paig-Tran E, Kleinteich T, Summers AP. 2013. The filter pads and filtration mechanisms of the devil rays: variation at macro and microscopic scales. *J. Morphol.* 274:1026–43
- Parks SE, Warren JD, Stamieszkin K, Mayo CA, Wiley D. 2012. Dangerous dining: surface foraging of North Atlantic right whales increases risk of vessel collisions. *Biol. Lett.* 8:57–60
- Pivorunas A. 1977. Fibro-cartilage skeleton and related structures of ventral pouch of balaenopterid whales. *J. Morphol.* 151:299–313
- Pivorunas A. 1979. Feeding mechanisms of baleen whales. *Am. Sci.* 67:432–40
- Potvin J, Goldbogen JA, Shadwick RE. 2009. Passive versus active engulfment: verdict from trajectory simulations of lunge-feeding fin whales *Balaenoptera physalus*. *J. R. Soc. Interface* 6:1005–25
- Potvin J, Goldbogen JA, Shadwick RE. 2010. Scaling of lunge feeding in rorqual whales: an integrated model of engulfment duration. *J. Theor. Biol.* 267:437–53
- Potvin J, Goldbogen JA, Shadwick RE. 2012. Metabolic expenditures of lunge feeding rorquals across scale: implications for the evolution of filter feeding and the limits to maximum body size. *PLOS ONE* 7:e44854
- Pyenson ND, Goldbogen JA, Shadwick RE. 2013. Mandible allometry in extant and fossil Balaenopteridae (Cetacea: Mammalia): the largest vertebrate skeletal element and its role in rorqual lunge feeding. *Biol. J. Linn. Soc.* 108:586–99
- Pyenson ND, Goldbogen JA, Vogl AW, Szathmary G, Drake RL, Shadwick RE. 2012. Discovery of a sensory organ that coordinates lunge feeding in rorqual whales. *Nature* 485:498–501
- Pyenson ND, Lindberg DR. 2011. What happened to gray whales during the Pleistocene? The ecological impact of sea-level change on benthic feeding areas in the North Pacific Ocean. *PLOS ONE* 6:e21295
- Pyke GH. 1984. Optimal foraging theory: a critical review. *Annu. Rev. Ecol. Syst.* 15:523–75
- Ray GC, Schevill WE. 1974. Feeding of a captive gray whale, *Eschrichtius robustus*. *Mar. Fish. Rev.* 36:31–38
- Rubenstein DI, Koehl MAR. 1977. Mechanisms of filter feeding: some theoretical considerations. *Am. Nat.* 111:981–94
- Sanderson SL, Cheer AY, Goodrich JS, Graziano JD, Callan WT. 2001. Crossflow filtration in suspension-feeding fishes. *Nature* 412:439–41
- Sanderson SL, Roberts E, Lineburg J, Brooks H. 2016. Fish mouths as engineering structures for vortical cross-step filtration. *Nat. Commun.* 7:11092
- Shadwick RE, Goldbogen JA, Potvin J, Pyenson ND, Vogl AW. 2013. Novel muscle and connective tissue design enables high extensibility and controls engulfment volume in lunge-feeding rorqual whales. *J. Exp. Biol.* 216:2691–701
- Simon M, Johnson M, Madsen PT. 2012. Keeping momentum with a mouthful of water: behavior and kinematics of humpback whale lunge feeding. *J. Exp. Biol.* 215:3786–98

- Simon M, Johnson M, Tyack P, Madsen PT. 2009. Behaviour and kinematics of continuous ram filtration in bowhead whales (*Balaena mysticetus*). *Proc. R. Soc. B* 276:3819–28
- Smith JM. 1978. Optimization theory in evolution. *Annu. Rev. Ecol. Syst.* 9:31–56
- Somero GN. 2000. Unity in diversity: a perspective on the methods, contributions, and future of comparative physiology. *Annu. Rev. Physiol.* 62:927–37
- Szewciw LJ, de Kerckhove DG, Grime GW, Fudge DS. 2010. Calcification provides mechanical reinforcement to whale baleen α -keratin. *Proc. R. Soc. B* 277:2597–605
- Webb PW, De Buffrénil V. 1990. Locomotion in the biology of large aquatic vertebrates. *Trans. Am. Fish. Soc.* 119:629–41
- Werth AJ. 2000. Feeding in marine mammals. In *Feeding: Form, Function and Evolution in Tetrapod Vertebrates*, ed. K Schwenk, pp. 475–514. New York: Academic
- Werth AJ. 2001. How do mysticetes remove prey trapped in baleen? *Bull. Mus. Comp. Zool.* 156:189–203
- Werth AJ. 2004. Models of hydrodynamic flow in the bowhead whale filter feeding apparatus. *J. Exp. Biol.* 207:3569–80
- Werth AJ. 2007. Adaptations of the cetacean hyolingual apparatus for aquatic feeding and thermoregulation. *Anat. Rec.* 290:546–68
- Werth AJ. 2011. Flow-dependent porosity of baleen. *Integr. Comp. Biol.* 51(Suppl. 1):e265 (Abstr.)
- Werth AJ. 2012. Hydrodynamic and sensory factors governing response of copepods to simulated predation by balaenid whales. *Int. J. Ecol.* 208913:1–13
- Werth AJ, Potvin J. 2016. Baleen hydrodynamics and morphology of cross-flow filtration in balaenid whale suspension feeding. *PLOS ONE* 11:e0150106
- Werth AJ, Straley JM, Shadwick RE. 2016. Baleen wear reveals intraoral water flow patterns of mysticete filter feeding. *J. Morphol.* 277:453–71
- Wiedenmann J, Cresswell KA, Goldbogen J, Potvin J, Mangel M. 2011. Exploring the effects of reductions in krill biomass in the Southern Ocean on blue whales using a state-dependent foraging model. *Ecol. Model.* 222:3366–79
- Wiley D, Ware C, Bocconcelli A, Cholewiak DM, Friedlaender AS, et al. 2011. Underwater components of humpback whale bubble-net feeding behaviour. *Behaviour* 148:575–602
- Williams R, Vikingsson GA, Gislason A, Lockyer C, New L, et al. 2013. Evidence for density-dependent changes in body condition and pregnancy rate of North Atlantic fin whales over four decades of varying environmental conditions. *ICES J. Mar. Sci.* 70:1273–80
- Williams TM. 1999. The evolution of cost efficient swimming in marine mammals: limits to energetic optimization. *Philos. Trans. R. Soc. Lond. B* 354:193–201
- Williams TM. 2001. Intermittent swimming by mammals: a strategy for increasing energetic efficiency during diving. *Am. Zool.* 41:166–76
- Williams TM. 2006. Physiological and ecological consequences of extreme body size in whales. In *Whales, Whaling, and Ocean Ecosystems*, ed. JA Estes, DP DeMaster, DF Doak, TM Williams, RL Brownell, pp. 191–201. Berkeley: Univ. Calif. Press
- Williams TM, Haun J, Davis RW, Fuiman LA, Kohin S. 2001. A killer appetite: metabolic consequences of carnivory in marine mammals. *Comp. Biochem. Physiol. A* 129:785–96
- Williamson G. 1973. Counting and measuring baleen and grooves of whales. *Sci. Rep. Whales Res. Inst.* 25:279–92
- Woodward BL, Winn JP. 2006. Apparent lateralized behavior in gray whales feeding off the central British Columbia coast. *Mar. Mamm. Sci.* 22:64–73
- Young S, Deméré TA, Ekdale EG, Berta A, Zellmer N. 2015. Morphometrics and structure of complete baleen racks in gray whales (*Eschrichtius robustus*) from the eastern North Pacific Ocean. *Anat. Rec.* 298:703–19